LIGHT ABSORPTION AND SIZE-SCALING OF LIGHT-LIMITED METABOLISM IN MARINE DIATOMS

Zoe Vanessa Finkel[1]
Department of Biology,
Dalhousie University,
Halifax, N.S.
Canada B3H 4J1

May 18, 2000

Running title: Size scaling of phytoplankton metabolism

[1] Current address: Dept. of Mathematics and Statistics, Queen's University, Kingston, Ontario, Canada K7L 3N6. E-mail: irwin@mast.queensu.ca, Ph: 613-533-2390, Fax: 613-533-2964.

ABSTRACT

Previous studies have found that the size scaling exponent of metabolic rates of unicellular algae often deviates from the exponent of $-1/4$ usually found for heterotrophs. This study confirms a significant linear relationship between log cell volume (μm^3) and log intrinsic growth rate (h^{-1}), carbon- normalised photosynthetic capacity and performanace (h^{-1}), and carbon-normalised respiratory rate (h^{-1}) for 8 marine centric diatoms under nutrient-saturated, light-limited conditions. The intrisic growth rate and carbon-normalised respiratory rate have size scaling exponents not significantly different from $-1/4$, while the carbon-specific photosynthetic rate deviates from $-1/4$. As expected, the optical absorption cross-section (m^2 mg chl-a^{-1}) decreases with cell volume. The size-dependence of optical properties due to pigment packaging provides a mechanistic model that explains the anomalous size scaling of the anabolic rates of unicellular phytoplankton.

INTRODUCTION

From bacteria to large mammals, body size is used to predict metabolic rates:

$$\frac{M}{C} = aV^b, \tag{1}$$

where a is a group-specific constant and b is the size scaling exponent of the relationship between the metabolic rate (M) normalised to biomass (for example C, carbon) and the size of the organism (e.g. cell volume V). Related organisms can have similar values of a but it is often quite variable (Chisholm, 1992). In contrast, b is commonly $-1/4$ when the metabolic rate is normalized to body mass (Peters, 1983). Since this paper focuses on carbon-normalized rates, this exponent will be referred to as the $-1/4$ rule. For cellular metabolism, the size scaling exponent is referred to as the $3/4$ law or Kleiber's rule.

Cullen et al. (1993) suggest cell size should be included in descriptions of phytoplankton growth intended for biogeochemical models. Cell size has been used to predict sinking rates, nutrient acquisition, light absorption, primary production and basic metabolism in phytoplankton (Joint and Pomroy, 1988; Agustí, 1991; Kiorboe, 1993; Tang, 1995). Several studies suggest that the size scaling exponent of metabolic rates in phytoplankton deviates from the $-1/4$ rule (Taguchi, 1976; Lewis, 1989; Sommer, 1989). Some of the variability in the size scaling of phytoplankton metabolism may be in response to environmental conditions. Banse (1976) predicted a change in the metabolic size scaling exponent with a degradation in growth conditions, and Schlesinger et al. (1981) found an increase in the size scaling exponent of the intrinsic growth rate of freshwater algae with decreasing light intensity.

Although many mechanisms have been suggested, the cause of size scaling of metabolic rates is unclear. Several hypotheses attribute the cause of size scaling of metabolic rates to morphological features and physiological processes not available to unicellular photoautotrophs (Kleiber, 1961; McMahon, 1973; Peters, 1983). For example, West et al. (1997) present a fractal model of the $-1/4$ rule based on the branching of tubular transport mechanisms of the mammalian cardiovascular system that is clearly not applicable to the unicellular protozoa (Beuchat, 1997). Banse (1976) suggests that the surface area to volume ratio may be responsible for the size scaling of metabolic rates in algae. As the volume of a cell of constant shape increases, the surface area to volume ratio decreases. This will alter rates of passive gas and nutrient diffusion per unit volume, resulting in a size scaling exponent of $-1/3$, not the commonly accepted value of $-1/4$ (Hemmingsen, 1960; Kleiber, 1961).

Light absorption may be responsible for the anomalous size scaling of the metabolic rates of phytoplankton (Finkel and Irwin 2000). Unlike heterotrophs, autotrophs depend on the absorption of light to drive their metabolic processes. Light absorption is a non-linear function of the composition and concentration of pigment and cell size (Morel and Bricaud, 1981; Kirk, 1994). The optical absorption

cross-section of phytoplankton cells (m^2 (mg chl-*a*)$^{-1}$) is given by

$$a^* = \frac{3}{2}\frac{a_s^* Q(\rho)}{\rho}, \tag{2}$$

where

$$Q(\rho) = 1 + 2\frac{e^{-\rho}}{\rho} + 2\frac{e^{-\rho} - 1}{\rho^2} \tag{3}$$

and

$$\rho = a_s^* c_i d, \tag{4}$$

where a_s^* (m^2 (mg chl-*a*)$^{-1}$) is the chlorophyll-specific absorption of the photosynthetic pigments in solution, Q and ρ are dimensionless, c_i ($10^9 \cdot$ pg chl-*a* μm^{-3}) is the intracellular chlorophyll-*a* concentration, and d is cell diameter (m).

An increase in cell size and/or intracellular pigment concentrations results in a decrease in a^*, referred to as the package effect (Morel and Bricaud, 1981). Assuming uniform c_i, and that the $-1/4$ size scaling of metabolic rates reported in heterotrophs still occurs in autotrophs, steeper size scaling is expected for the anabolic rates of light-limited unicellular autotrophs (Finkel and Irwin, 2000). The exact nature of the size scaling of the anabolic rates depends on the relationship between c_i and cell size. The general idea is that the package effect modifies the size scaling of light-limited metabolic rates by changing a^*, thereby altering the amount of energy available for the metabolic reactions.

This study addresses two questions. First, does the size scaling exponent of the intrinsic growth rate, carbon-specific rate of photosynthesis, and respiration deviate from the $-1/4$ rule under sub-optimal growth conditions, specifically sub-saturating irradiance? Second, can the effect of pigment packaging on the light-absorptive properties of the cells explain anomalous size scaling in photosynthesis? To address these questions, photosynthesis, respiration, growth, the efficiencies of growth and photosynthesis, and light absorptive properties were quantified for eight diatom species that range in size from approximately 10 to 250000 μm^3. A list of symbols used is provided in Table 1.

MATERIALS AND METHODS

Phytoplankton cultures and growth conditions

Eight centric diatom species were chosen, representing a wide spectrum of cell sizes: *Chaetoceros calcitrans* (CCMP1315), *Thalassiosira pseudonana* (CCMP1335), *Chaetoceros* sp. (no official identification), *Thalassiosira weissflogii* (CCMP1336), *Hyalodiscus* sp. (CCMP1679), *Planktoniella sol*

(CCMP1608), *Coscinodiscus* sp. (CCMP312), and *Coscinodiscus* sp. (CCMP1583). All species had numerous discoid chloroplasts, except for the *Chaetoceros* spp. which have one or more sheet-like plastids (Round et al., 1990). All cultures were obtained from the Provasoli-Guillard National Center for the Culture of Marine Phytoplankton (CCMP) with the exception of *Chaetoceros* sp., which was isolated from the Huntsman Marine Science Center in St. Andrews, New Brunswick (J. Jellett pers. comm.). Cultures were grown in 2.8-litre glass Fernbach flasks at 20°C in $f/2$ enriched, 0.45-μm filtered Bedford Basin sea-water (Guillard and Ryther, 1962). The cultures were illuminated by a combination of broad spectrum Sylvania fluorescent tubes F30T12 and F15T12D to a continuous photon flux density of 25 μmol photon m^{-2} s^{-1} as measured by a biospherical light sensor placed in the culture vessel filled with media. Cultures were manually agitated approximately once per day.

Semi-continuous culture technique (Ukeles, 1973) kept the cultures in exponential growth for a minimum of three generations prior to the photosynthetic experiments. The exponential growth rate was considered reached once the growth rate no longer increased with an increased rate of influx of new culture media. To minimize bacterial contamination careful aseptic technique was used in the maintenance and growth of all cultures.

Estimates of phytoplankton biomass

The diameter (d) and height (h) of the diatoms were measured under the microscope with an ocular ruler. For each species, between 80-100 measurements were made of each dimension. The average cell volume was calculated from the average cell height and average square radius, assuming all cells to be cylinders. Two sets of cell size measurements were combined to derive an average estimate of cell volume associated with the growth rate. *Hyalodiscus sp.* doublets were treated as single cells because doublets were surrounded by a thick mucilaginous coating.

Chlorophyll *a* concentrations were determined fluorometrically, in triplicate, from samples concentrated on filters and then extracted for 24 or more hours in ice-cold 90% acetone (Holm-Hansen et al., 1965). In addition, HPLC analysis provided estimates of the concentration of chlorophylls, carotenoids and other accessory pigments in a subset of the samples. Samples were run on a Beckman C18, reversed phase, 3-mm Ultrasphere column using the solvent gradient system of Head and Horne (1993). Fluorometer estimates were calibrated with HPLC determinations of chlorophyll *a*. Carbon content was determined with a Perken-Elmer 2400 CHN Elemental Analyzer. Phytoplankton were filtered onto pre-combusted GF/F filters and placed in the freezer or desiccator until analysis.

The number of cells per unit volume for the five smallest diatoms was determined using the Levy Improved Neubauer and American Optical Brightline haemacytometers (both 0.2 mm deep). For each cell

density estimate a minimum of four slides were counted. The cell densities of the three larger clones were determined using a Sedwick-Rafter chamber, divided into 11 fields of view. Generally, two to four chambers were examined. When practical, enough cells were counted to keep the coefficient of variation of the mean population estimate below 20%. The $\log_e$ growth rate (μ in h^{-1}) was determined using linear regression as described by Guillard (1973).

Photosynthesis-irradiance (PI) experiments

Photosynthetic rate was estimated with $NaH^{14}CO_3$, following Irwin et al. (1986), with some modifications. Each experiment employed 30 light bottles and 3 dark bottles, which were filtered after a 1 h incubation at the experimental irradiance. Inorganic carbon was removed by placing the filters over concentrated HCl for 20-30 minutes prior to placement in scintillation fluid. Disintegrations per minute, measured by a Beckman LS 5000 CE liquid scintillation counter, were converted to photosynthetic rates as described by Geider and Osborne (1992). A three-parameter hyperbolic tangent function was fitted to the PI data:

$$P(I) = P_{\max} \tanh(\alpha I / P_{\max}) - {}^{14}CR \tag{5}$$

where I is the irradiance in μmol quanta $m^{-2}s^{-1}$, $P_{\max}$ is the photosynthetic capacity in mg C h^{-1}, α is the photosynthetic efficiency in mg C h^{-1} μmol quanta $m^{-2}s^{-1}$, and ${}^{14}CR$ represents the dark respiratory rate in mg C h^{-1} (Platt and Jassby, 1976). The ratio $\frac{P_{\max}}{\alpha} = I_k$ was calculated to determine the irradiance at which photosynthetic capacity is reached. In all cases, I_k was higher than the growth irradiance, verifying that all experimental species experienced light limitation.

Oxygen consumption

Changes in oxygen concentration were determined in the dark by an ENDECO oxygen electrode system calibrated with a series of Winkler titrations following the method of Levy et al. (1977) and Kepkay et al. (1997). Electrodes were pulsed every 5 minutes over a 24-30 hour period in a one litre jacketed glass vessel held at 20°C. The rate of oxygen consumption changed over the course of the incubation. Due to a variable rate of oxygen consumption over the first several hours, the rate of oxygen consumption over the last 14 hours of the incubation is presented. As in Blasco et al. (1982) a respiratory quotient of one was used to convert moles O_2 (moles C $\cdot$ h)$^{-1}$ to h^{-1}.

Phytoplankton absorption measurements

The ratio of incident irradiance to transmitted irradiance, the optical density, was obtained from a Shimadzu UV-2101 PC spectrophotometer equipped with an integrating sphere. Phytoplankton cultures were filtered

under low pressure onto GF/F filters. The same volume of filtrate was filtered under low pressure onto a second GF/F filter. The two filters were placed in the spectrophotometer in special filter holders, with the filtrate collected on the second filter serving as a blank. The absorption of the phytoplankton culture and detritus was estimated using the methods described in Hoepffner and Sathyendranath (1993) and references therein. A correction factor was applied to the optical densities determined from the filters. The correction factor (path-length amplification or β-factor) was determined by fitting a two-parameter quadratic function to the experimentally determined optical density data from filters and in suspension, as described by Mitchell (1990). Spectrally averaged absorption ($\bar{a}$) was calculated by integrating the absorption over all measured wavelengths and dividing by the number of wavelengths measured

$$\bar{a} = \frac{\int_{400}^{700} a(\lambda)\ d\lambda}{\int_{400}^{700} d\lambda}. \tag{6}$$

Quantum yield

The quantum yield of photochemistry (ϕ_f) was estimated from the measurement of *in vivo* dark-adapted fluorescence (F_0) and 3-[3,4-dichlorophenyl]-1,1-dimethyl urea (DCMU) enhanced fluorescence (F_m) following Olson et al. (1996) where

$$\phi_f = \frac{F_m - F_0}{F_m}.$$

The quantum yield of carbon fixation (ϕ_p) is calculated by

$$\phi_p = 0.231\alpha/\bar{a}, \tag{7}$$

where 0.231 converts mg carbon to moles, hours to seconds, and μmol quanta to moles of quanta (Platt and Jassby, 1976). Note that ϕ_p may be an over-estimate of the true value because α may provide an estimate closer to gross than net photosynthesis. The effect of the spectral quality of the tungsten light on photosynthetic efficiency was corrected according to Kyewalyanga (1997).

At the growth irradiance, the quantum yield of growth (ϕ_μ), was calculated following a simplified form of the equation provided by Sosik and Mitchell (1991):

$$\phi_\mu = 4.32 \cdot 10^7 \frac{k\theta}{a^* I} \tag{8}$$

where μ is the growth rate (h^{-1}), θ is the C to chlorophyll *a* ratio (mg:mg), a^* is the chlorophyll *a*-specific absorption coefficient in m^2 mg chl-a^{-1}, I is the irradiance in the growth incubator in μmoles m^{-2} s^{-1}, and $4.32 \cdot 10^7$ is the product of 12000 which is a constant that converts mg carbon into moles carbon and 3600 which converts the growth rate from s^{-1} to h^{-1}. The quantum yield was corrected to account for variation in the spectrum of the fluorescent lights in the growth chamber as described for the tungsten lamp previously. Spectral irradiance values for the fluorescent tubes were provided by Sylvania Ltd.

Regression analysis and the determination of size scaling exponents

According to the allometric power law (Equation 1), metabolic rates can be described by an expression relating cell size to an exponent. Least squares regression analysis (OLS) and reduced major axis regression (RMA) were both performed to determine the size-scaling exponent and intercept. According to Ricker (1973) and LaBarbera (1989) RMA is preferable to OLS, although results will converge as the correlation coefficient increases. The RMA regression minimizes the squared normal deviates, following Kermack and Haldane (1950) and York (1966). OLS regression parameters are more commonly reported than RMA regression parameters. For consistency, only the OLS regression coefficients are referred to in the text. Regression coefficients will be referred to as statistically significant at the 95% significance level and means are reported with their standard errors.

RESULTS

Cell size and cellular composition

The eight species in this study span an approximate 25000-fold range in volume, from just over 10 to over 250000 μm^3. All species have similar pigment composition. Chlorophyll *a* and fucoxanthin represent 70-89% of the total cellular pigment content. Chlorophyll *c*, β-carotene, and diadinoxanthin account for the majority of the remaining pigment. Pigment and carbon content per cell, had positive, statistically significant relationships with cell volume (Table 2). Intracellular carbon appears to be approximately linearly related to cell volume. In constrast, intracellular chlorophyll-*a* content has a size-scaling exponent of 0.69 ± 0.04, resulting in an increase in the carbon-to-chlorophyll-*a* ratio (θ) with cell volume. The increase in θ results in systematically larger size-scaling exponents associated with the chlorophyll-*a* versus the carbon-normalized metabolic and physiological rates. The subsequent allometric analyses focus on the carbon normalised rates, indicated by a superscript C.

The size-scaling of metabolic processes

The size scaling exponents associated with the cellular composition, metabolic rates, and physiological parameters of the marine diatoms are presented in Table 2. The intrinsic growth rates μ of the diatom clones span an 7.8-fold range, with doubling times from 33 hours for the smallest clone to 258 hours for the second largest clone. The size scaling exponent of μ is -0.22 ± 0.03, which is not significantly different from the $-1/4$ rule (Figure 1A).

The carbon-specific respiratory rates, ${}^{14C}R^C$ and ${}^{O}R^C$, decrease similarly to μ with cell volume (Figure 1B). Oxygen electrode estimates of respiration are on average approximately an order of magnitude

higher than the ^{14}C estimates, but the size scaling of oxygen consumption supports and reinforces the size-dependence found for the ^{14}C estimates of respiratory loss. Note that the average $^{14}CR^C$ for *T. pseudonana* was negative, and therefore excluded from the analysis.

In constrast to μ and R^C, the size scaling of $P^C_{\max}$ and P^C_k significantly differ from the $-1/4$ rule (Figure 1C). Carbon-specific photosynthetic capacity ($P_{\max}$) and photosynthetic performance (P_k) have size scaling exponents significantly less than those associated with growth and respiratory processes.

Phytoplankton absorption parameters

The chlorophyll-*a*-specific absorption spectra suggest that the size scaling of light absorption is due to the package effect. As the package effect increases the absorption spectra becomes flattened, resulting in a decrease in the ratio of the maximum absorption peaks. The absorption spectra of the diatom clones cluster in two distinct groups (Figure 2A). *Chaetoceros calcitrans, Thalassiosira pseudonana,* and *Chaetoceros* sp., the three smallest species examined, have high $\bar{a}^*$, and high ratios of blue to red absorption. The four larger diatoms: *Cosinodiscus* spp, *Hyalodiscus* sp., and *Thalassiosira weissflogii* have lower values of $\bar{a}^*$ and have lower ratios of blue to red absorption. *P. sol* has a much higher $\bar{a}^*$ compared with other diatoms of comparable size, likely due to its large mucilaginous wing, and was therefore excluded from the analysis.

As mentioned earlier, changes in pigment composition, pigment concentration and cell size can alter the optical absorption cross-section through the package effect. Pigment composition was nearly constant between the different diatom species. This suggests a combination of cell size and pigment concentration control the approximate 2-fold decrease in the spectrally-averaged optical absorption cross-section with cell size (Figure 2B). Pigment concentration per unit volume, c_i, decreases with cell volume.

The photosynthetic parameters, $P^C_{\max}$ and P^C_k are highly correlated with the spectrally-averaged optical absorption cross-section (Figure 3A). Light-limited P_k is the product of the incident irradiance, $\bar{a}$ and the maximum quantum yield of photosynthesis. The effect of size-dependent $\bar{a}^C$ on the size scaling exponent of light-limited P^C_k can be predicted by incorporating the $-1/4$ size scaling of metabolism into the bio-optic model of photosynthesis (Finkel and Irwin, 2000). This can be done by decomposing $\phi_{\max}$ into $\alpha^C/\bar{a}^C$, and constructing a hybrid α^C_{AB} that includes not only the biophysical properties of absorption but also the size scaling of metabolism. For example α^C_{AB} could be expressed as $\alpha^C_B \cdot \alpha^C_A$, where $\alpha^C_B = \phi_{\max} \cdot \bar{a}^C$ incorporates the biophysics of light absorption and photosynthesis (Eqns. 2-4) and α^C_A introduces the $-1/4$ size scaling of metabolic rates (Eq. 1). The product α^C_{AB} is only one of numerous ways to incorporate the size scaling of metabolism into a bio-optical description of photosynthesis. A direct comparison of the predictions from this combined allometric-bio-optic model and P^C_k is provided in Figure 3B. For details on the values used for the parameters see Finkel and Irwin (2000). The agreement

between the model (solid line) and the data (filled circles) is qualitatively superior to the simple $-1/4$ rule (dashed line). There is a shallower slope for small cells and the curve is slightly concave down reflecting the changing package effect with increasing cell size.

The efficiency of photosynthesis and growth

Three different estimates of quantum yield show different degrees of size-dependence. The maximum quantum yield of photochemistry, ϕ_f, is independent of cell size and is close to maximum reported values with a mean of 0.637 (Figure 4A). In contrast, the quantum yield of photosynthesis (ϕ_p) is significantly lower than reported maximum values, ranging from 0.014 to 0.070 moles of carbon produced per mole of photons absorbed (a 5-fold range), and has a statistically significant negative relationship with cell volume (Figure 4B). Similar to ϕ_p, the quantum yield of growth (ϕ_μ) has a 4.5-fold range in values, from 0.02 to 0.09, but in contrast to ϕ_p, ϕ_μ is not size-dependent (Figure 4C).

DISCUSSION

This study confirms the significant linear relationship between log cell volume (μm^3) and log of the metabolic rates of the marine centric diatoms under nutrient-saturated, light-limited conditions. The intrisic growth rate and carbon-normalised respiratory rate have size scaling exponents not significantly different from $-1/4$, in agreement with Tang (1995) and Tang and Peters (1995). In constrast, carbon-specific P_k and $P_{\max}$ deviate from the $-1/4$ rule, in agreement with Taguchi (1976). These size scaling coefficients are significantly less than $-1/4$, contrary to the suggestion made by Banse (1976) of an increase in the size scaling exponent with sub-optimal growth conditions.

Decreases in the optical absorption cross-section with cell size can explain the anomalously steep size scaling exponent associated with light-limited photosynthetic performance. The diatom cells in this study exhibited a size-dependent decrease in $\bar{a}^*$ due to the increased self-shading of pigments within the cell with increasing cell volume (Morel and Bricaud, 1981; Kirk, 1994). The decrease in $\bar{a}^*$ results in a decrease in P_k^C with cell size under sub-saturating light intensities. An allometric-bio-optic model that combines the effect of size scaling in $\bar{a}^*$ due to the package effect with the $-1/4$ size scaling of metabolism can predict the observed anomalously low size scaling exponent associated with P_k^C (Finkel and Irwin 2000). This prediction assumes $\phi_{\max}$, pigment composition and pigment concentration are independent of cell size.

In general, this study and previous evidence indicate that the quantum yield of photosynthesis and growth are independent of size (Geider et al., 1986). The quantum yield of photosynthesis or carbon assimilation (ϕ_p) provides an estimate of the efficiency of conversion of absorbed light energy into carbon

products under low light. Theoretically, algae grown under low light and high nutrient concentrations should have a constant ϕ_p, close to the theoretical maximum ($\phi_{\max}$), between 0.1 to 0.125 (Geider et al. 1986; Kirk, 1994). In the present study ϕ_f and ϕ_μ are independent of cell size, but ϕ_p is variable and tends to decrease with increasing cell size. The size scaling of ϕ_p may be an artifact due to the method of measurement. The incorporation of ^{14}C can provide an ambiguous estimate of photosynthesis somewhere between net and gross photosynthesis depending on the ratio of the incubation to generation time of the organism (Li and Goldman, 1981). Alternatively the size scaling of ϕ_p may be due to the decrease in the surface area-to-volume (SA/V) ratio with cell size. The decrease in SA/V results in lower rates of passive nutrient diffusion per unit volume, and therefore higher metabolic energy expenditure for equivalent nutrient capture. Higher capital costs associated with nutrient assimilation and light capture of the larger cells could potentially contribute to the size-scaling of ϕ_p. Even given the size scaling of ϕ_p, the lack of size scaling associated with the quantum yield of growth and photochemistry supports the assumption of a constant $\phi_{\max}$, and previous evidence that energetic efficiencies are independent of an organism's size (Peters 1981).

The diatom cells all have very similar pigment composition, leaving pigment concentration and cell size resposible for the variation in the optical absorption cross-section. Intracellular chlorophyll-*a* concentrations (c_i) tend to decrease with cell volume. The decrease in c_i with cell size is a pattern common to many phytoplankton taxa (Agustí, 1991). This pattern suggests there is evolutionary pressure to decrease intracellular pigment concentration with cell size to optimise the optical absorption cross-section. Compared with constant c_i, an inverse relationship with cell size results in a moderation of the increase in the package effect with cell size. Despite the decrease in c_i with cell size there is still an increase in the package effect and a resulting decrease in $\bar{a}^*$ with cell size in the light-limited diatoms.

The increase in the package effect with cell size may result in the size scaling of the number of photosynthetic units n (O_2/chl-*a*). This is because at the same c_i the probability each chlorophyll-*a* molecule will intercept and absorb an incident photon decreases with increasing cell size. For example, Sukenik et al. (1990) found n decreases when *Dunaliella tertiolecta* is transferred from a high light to a low light environment. This demonstrates that an increase in c_i which is likely resposible for an increase in the package effect results in a decrease in the number of photosynthetic units. There is an analogous relationship between the physiological response associated with photoacclimation and that of cells of different sizes grown under low light. Consider two cells identical in every respect but size, the larger cell will intercept less incident irradiance per unit of pigment than the smaller cell. It is not unreasonable to suggest that larger cells, like the cells exposed to lower irradiance, will experience a more acute package effect and have lower values of n than the smaller cells which intercept relatively more of the incident

irradiance per molecule of chlorophyll-*a*.

The size scaling of the number of photosynthetic units can explain the anomalous size scaling of both P_k and $P_{\max}$ under light-limiting conditions. Unlike P_k^C, $P_{\max}^C$ does not depend directly on the optical absorption cross-section (Falkowski, 1981). Following the notation described in Falkowski and Raven (1997), it is evident that $P_{\max}$, P_k ($\approx \alpha I$, assuming I is sub-saturating), and a^* can all depend on n:

$$\begin{aligned} P_{\max}^* &= \frac{n}{\tau} \\ \alpha^* &= n\sigma_{\text{PSII}} \\ a^* &= n\sigma_{\text{PSU}}, \end{aligned}$$

where τ^{-1} is the rate at which electrons are transferred from H_2O to CO_2 at steady state (s^{-1}), σ_{PSII} is the cross-section of photosystem II (m^2 mole quanta^{-1}), and σ_{PSU} is the cross-section of the photosynthetic unit (m^2 mole PSU^{-1}). Assuming τ, σ_{PSII} and σ_{PSU} remain constant, a decrease in n with cell size will result in a corresponding decrease in a^*, P_k^C, and $P_{\max}^C$. This decrease in n can also account for the strong correlation found between $\bar{a}^C$ and the photosynthetic parameters.

An organism's size is often a good predictor of its metabolic rate. For many different taxonomic groups metabolic rate follows the $-1/4$ rule. Phytoplankton cover an extremely large size range from diameters of less than a μm to over a millimeter. Over this size range the $-1/4$ rule predicts an approximate 18-fold range in the biomass-specific metabolic rates. This suggests phytoplankton cell size in combination with the $-1/4$ rule could be used successfully to predict metabolic rates such as primary production. This study confirms that the allometric power law is a good model for the prediction of light-limited nutrient-saturated metabolic processes in marine diatoms. However, the $-1/4$ rule does not adequately describe the size-dependence of light-limited anabolic rates which appear to be influenced by pigment packaging. If an allometric model is to be used to predict growth rates and primary production in aquatic ecosystems, more work is required to understand the role of light absorption and pigment packaging on the size scaling of metabolic rates on different taxonomic groups of phytoplankton under a variety of growth conditions.

ACKNOWLEDGEMENTS

This work was supported by a Dalhousie graduate scholarship. I acknowledge the support of T. Platt and S. Sathyendranath, and also thank P. Kepkay, J. Jellett, B. Irwin, W.K.W. Li, V. Stuart, E. Head, V. Lutz, R. Campbell, J. Bugden, and A. Irwin.

REFERENCES

Agustí, S. 1991. Allometric scaling of light absorption and scattering by phytoplankton cells. *Canadian Journal of Fisheries and Aquatic Sciences* **48**:763–767.

Banse, K. 1976. Rates of growth, respiration and photosynthesis of unicellular algae as related to cell size – A review. *Journal of Phycology* **12**:135–140.

Beuchat, C. 1997. Allometric scaling laws in biology. *Science* **278**:371.

Blasco, D., T. T. Packard, and P. C. Garfield. 1982. Size dependence of growth rate, respiratory electron transport system activity, and chemical composition in marine diatoms in the laboratory. *Journal of Phycology* **18**:58–63.

Chisholm, S. W. 1992. Phytoplankton size. In P. G. Falkowski and A. D. Woodhead, editors, *Primary productivity and Biogeochemical cycles in the sea*, pages 213–237. Plenum Press.

Cullen, J. J., R. J. Geider, J. Ishizaka, D. A. Kiefer, J. Marra, E. Sakshaug, and J. A. Raven. 1993. Toward a general description of phytoplankton growth for biogeochemical models. In G. T. Evans and M. J. R. Fasham, editors, *Towards a Model of Ocean Biogeochemical Processes*, volume I 10 of *NATO ASI Series*, pages 153–176. Springer-Verlag.

Falkowski, P. G. 1981. Light-shade adaptation and assimilation numbers. *Journal of Plankton Research* **3**:203–216.

Falkowski, P. G. and J. Raven. 1997. *Aquatic Photosynthesis.* Blackwell Science.

Finkel, Z. V. and A. J. Irwin. 2000. Modeling size-dependent photosynthesis: light absorption and the allometric rule. *J. theor. Biol.* **204**:361–369.

Geider, R. J. and B. A. Osborne. 1992. *Algal photosynthesis.* Chapman and Hall.

Geider, R. J., T. Platt, and J. A. Raven. 1986. Size dependence of growth and photosynthesis in diatoms: A synthesis. *Marine Ecology Progress Series* **30**:93–104.

Guillard, R. 1973. Division rates. In J. Stein, editor, *Handbook of phycological methods: culture methods and growth measurements*, pages 289–312. Cambridge University Press.

Guillard, R. R. L. and J. H. Ryther. 1962. Studies of marine planktonic diatoms. I. *Cyclotella nana* Hustedt and *Detonula confervacea* Cleve. *Canadian Journal of Microbiology* **8**:229–239.

Head, E. J. H. and E. P. W. Horne. 1993. Pigment transformation and vertical flux in an area of convergence in the North Atlantic. *Deep-Sea Research II* **40**:329–346.

Hemmingsen, A. M. 1960. Energy metabolism as related to body size and respiratory surfaces, and its evolution. *Reports of the Steno Memorial Hospital* **9**:15–22.

Hoepffner, N. and S. Sathyendranath. 1993. Determination of the major groups of phytoplankton pigments from the absorption spectra of total particulate matter. *Journal of Geophysical Research* **98**:22,789–22,803.

Holm-Hansen, O., C. J. Lorenzen, R. W. Holmes, and J. D. H. Strickland. 1965. Fluorometric determination of chlorophyll. *Journal du Conseil (Conseil Permanent International pour l'Exploration de la Mer)* **30**:3–15.

Irwin, B., C. Caverhill, P. Dickie, E. Horne, and T. Platt. 1986. Primary productivity on the Labrador Shelf during June and July 1984. *Canadian Data Report of Fisheries and Aquatic Sciences* **577**.

Joint, I. and A. Pomroy. 1988. Allometric estimation of the productivity of phytoplankton assemblages. *Marine Ecology Progress Series* **47**:161–168.

Kepkay, P. E., J. F. Jellett, and S. E. H. Niven. 1997. Respiration and the carbon-to-nitrogen ratio of a phytoplankton bloom. *Marine Ecology Progress Series* **150**:249–261.

Kermack, K. A. and J. Haldane. 1950. Organic correlation and allometry. *Biometrika* **37**:30–41.

Kiorboe, T. 1993. Turbulence, phytoplankton cell size, and the structure of pelagic food webs. *Advances in Marine Biology* **29**:1–72.

Kirk, J. T. O. 1994. *Light and Photosynthesis in Aquatic Ecosystems.* Cambridge University Press, 2^{nd} edition.

Kleiber, M. 1961. *The fire of life: an introduction to animal energetics.* John Wiley and Sons.

Kyewalyanga, M. 1997. *Spectral-dependence of photosynthesis in marine phytoplankton.* Ph.D. thesis, Dalhousie University.

LaBarbera, M. 1989. Analyzing body size as a factor in ecology and evolution. *Annual Review of Ecological Systems* **20**:97–117.

Levy, E. M., C. C. Cunningham, C. D. W. Conrad, and J. D. Moffatt. 1977. The determination of dissolved oxygen in seawater. *Bedford Institute of Oceanography Report Series* **BI-R-77-9**:16.

Lewis, W. M., Jr. 1989. Further evidence for anomalous size scaling of respiration in phytoplankton. *Journal of Phycology* **25**:395–397.

Li, W. K. W. and J. C. Goldman. 1981. Problems in estimating growth rates of marine phytoplankton from short-term ^{14}C assays. *Microbial Ecology* **7**:113–121.

McMahon, T. A. 1973. Size and shape in biology. *Science* **179**:1201–1204.

Mitchell, B. G. 1990. Algorithms for determining the absorption coefficient of aquatic particulates using the quantitative filter technique (QFT). *Proceedings of the Society of Photo-Optical Instrumentation Engineers. Ocean Optics X.* **1302**:137–148.

Morel, A. and A. Bricaud. 1981. Theoretical results concerning light absorption in a discrete medium, and application to specific absorption of phytoplankton. *Deep-Sea Research 1* **28A**:1375–1393.

Olson, R. J., A. M. Chekalyuk, and H. M. Sosik. 1996. Phytoplankton photosynthetic characteristics from fluorescence induction assays of individual cells. *Limnology and Oceanography* **41**:1253–1263.

Peters, R. H. 1983. *The ecological implications of body size.* Cambridge University Press.

Platt, T. and A. D. Jassby. 1976. The relationship between photosynthesis and light for natural assemblages of coastal marine phytoplankton. *Journal of Phycology* **12**:421–430.

Ricker, W. E. 1973. Linear regressions in fisheries research. *Journal of the Fisheries Research Board of Canada.* **30**:409–434.

Round, F. E., R. M. Crawford, and D. G. Mann. 1990. *The Diatoms: biology and morphology of the genera*. Cambridge University Press.

Schlesinger, D. A., L. A. Molot, and B. G. Shuter. 1981. Specific growth rates of freshwater algae in relation to cell size and light intensity. *Canadian Journal of Fisheries and Aquatic Sciences* **38**:1052–1058.

Sommer, U. 1989. Maximal growth rates of Antarctic phytoplankton: Only weak dependence on cell size. *Limnology and Oceanography* **34**:1109–1112.

Sosik, H. M. and B. G. Mitchell. 1991. Absorption, fluorescence, and quantum yield for growth in nitrogen-limited *Dunaliella tertiolecta. Limnology and Oceanography* **36**:910–921.

Sukenik, A., J. Bennett, A. Mortain-Bertrand, and P. G. Falkowski. 1990. Adaptation of the photosynthetic apparatus to irradiance in *Dunaliella tertiolecta. Plant Physiol.* **92**:891–898.

Taguchi, S. 1976. Relationship between photosynthesis and cell size of marine diatoms. *Journal of Phycology* **12**:185–189.

Tang, E. P. Y. 1995. The allometry of algal growth rates. *Journal of Plankton Research* **17**:1325–1335.

Tang, E. P. Y. and R. H. Peters. 1995. The allometry of algal respiration. *Journal of Plankton Research.* **17**:303–315.

Ukeles, R. 1973. Continuous culture – a method for the production of unicellular algal foods. In J. Stein, editor, *Handbook of phycological methods: culture methods and growth measurements*, pages 233–254. Cambridge University Press.

West, G. B., J. H. Brown, and B. J. Enquist. 1997. A general model for the origin of allometric scaling laws in biology. *Science* **276**:122.

York, D. 1966. Least-squares fitting of a straight line. *Canadian Journal of Physics* **44**:1079–1086.

Table 1: List of symbols. The superscripts * and C refer to normalization of the parameter by mg chl-*a* or mg carbon.

Symbol	Description	Units
$\bar{a}$	Spectrally averaged absorption cross-section	m^2
α	Photosynthetic efficiency	mg C h^{-1} μmol photons m^{-2} s^{-1}
C	Intracellular carbon content	μg
c_i	Intracellular chl-*a* concentration	pg chl-*a* μm^{-3}
Chl	Total intracellular chlorophyll *a* content	pg
I	Available irradiance	μmol photons m^{-2} s^{-1}
I_k	Ratio $P_{\max}/\alpha$	μmol photons m^{-2} s^{-1}
μ	Intrinsic growth rate	h^{-1}
$P_{\max}$	Photosynthetic capacity	mg C h^{-1}
P_k	Photosynthetic performance	mg C h^{-1}
ϕ_f	Quantum yield of photochemistry	dimensionless
ϕ_μ	Quantum yield of growth	dimensionless
ϕ_p	Quantum yield of photosynthesis	dimensionless
${}^{14}CR$	Respiration derived from P-I curve	mg C h^{-1}
${}^{O}R$	Respiration derived from oxygen consumption	mg C h^{-1}
θ	Carbon-to-chlorophyll *a* ratio	wt:wt
V	Cell volume	μm^3

Table 2: Ordinary least squares (OLS) and reduced major axis (RMA) regression coefficients associated with the relationship between the log of the cellular components, metabolic and physiological parameters and log cell volume. Symbols are defined in Table 1.

		OLS regression coefficients		RMA regression coefficients		
Equation	n	intercept (±se)	slope (±se)	intercept (±se)	slope (±se)	r^2
Chl	16	-1.678 ± 0.135	0.690 ± 0.036	-1.707 ± 0.083	0.699 ± 0.035	0.96
C	8	-6.864 ± 0.146	0.963 ± 0.060	-6.816 ± 0.253	0.949 ± 0.069	0.97
θ	8	1.055 ± 0.119	0.193 ± 0.049	1.065 ± 0.204	0.189 ± 0.056	0.66
c_i	16	-1.678 ± 0.136	-0.310 ± 0.035	-1.659 ± 0.083	-0.313 ± 0.035	0.84
P^C_{max}	24	-0.168 ± 0.170	-0.440 ± 0.046	-0.108 ± 0.108	-0.457 ± 0.046	0.81
P^C_k	24	-0.153 ± 0.177	-0.453 ± 0.048	-0.087 ± 0.113	-0.473 ± 0.048	0.80
${}^{14\mathrm{C}}R^C$	22	-2.080 ± 0.112	-0.284 ± 0.030	-2.070 ± 0.069	-0.288 ± 0.029	0.82
${}^{O}R^C$	24	-1.352 ± 0.292	-0.290 ± 0.077	-1.216 ± 0.195	-0.329 ± 0.084	0.39
k_e	8	-1.172 ± 0.113	-0.220 ± 0.030	-1.168 ± 0.064	-0.221 ± 0.026	0.90
$\bar{a}^*$	7	-1.585 ± 0.030	-0.077 ± 0.012	-1.585 ± 0.052	-0.077 ± 0.014	0.85
$\bar{a}^C$	7	-2.476 ± 0.137	-0.359 ± 0.056	-2.500 ± 0.233	-0.352 ± 0.065	0.85
ϕ_{ps}	7	-1.045 ± 0.075	-0.138 ± 0.031	-1.048 ± 0.129	-0.137 ± 0.036	0.74

Figure Captions

Figure 1.

Size-scaling of growth, respiration and photosynthesis with standard error bars. Standard error was not included for volume because in most cases the error was smaller than the data point.

A) Instantaneous growth rate ($\mu \pm$se) at the growth irradiance.

B) Carbon-specific respiration. Indirect estimate of respiration from the photosynthesis-irradiance curve ($^{14C}R^C$) is represented by circles, the oxygen estimate of respiration ($^{O}R^C$) is represented by squares. The size-scaling regression lines are represented by a dotted line for $^{14C}R^C$, and a solid line for $^{O}R^C$.

C) Carbon-specific photosynthesis. Photosynthetic capacity ($P^C_{\max}$) is represented by the circles, and photosynthetic performance (P^C_k) is represented by the squares. The size scaling regression lines are represented by a solid line for $P^C_{\max}$ and a dashed line for P^C_k.

Figure 2.

Size-dependence of light absorption.

A) Chlorophyll *a*-specific absorption spectra. The upper group of three heavy lines are *Chaetoceros calcitrans* (dotted, ···), *Cyclotella* (solid, –), and *Chaetoceros* sp. (dashed, --). The lower group of four thin lines are *Thalassiosira* (dashed, --), *Hyalodiscus* (solid, –), *Coscinodiscus* 312 (dotted, ···), and *Coscinodiscus* 1583 (dash-dotted, –·–·). *Planktoniella sol* was excluded.

B) Size-dependence of the average chlorophyll *a*-specific absorption coefficient ($\bar{a}^*$). The outlier *Planktoniella sol* is shown as a filled box. Error bars represent one standard error.

Figure 3.

A) Photosynthesis-absorption relationship showing P^C_k as a function of $\bar{a}^C$. Error bars represent one standard error.

B) The prediction of carbon-specific photosynthesis using a combination of the $-1/4$ rule and the size dependence of light absorption due to the pacakge effect (solid line) together with the $-1/4$ allometric rule (dashed line) and experimental data, P^C_k (open circles). Figure redrawn from Finkel and Irwin (2000).

Figure 4.

The quantum yield of photosynthesis and growth with standard error bars.

A) Quantum yield of photochemistry (ϕ_f).

B) Size-dependence of the quantum yield of ^{14}C assimilation (ϕ_p).

C) Quantum yield of growth (ϕ_μ).

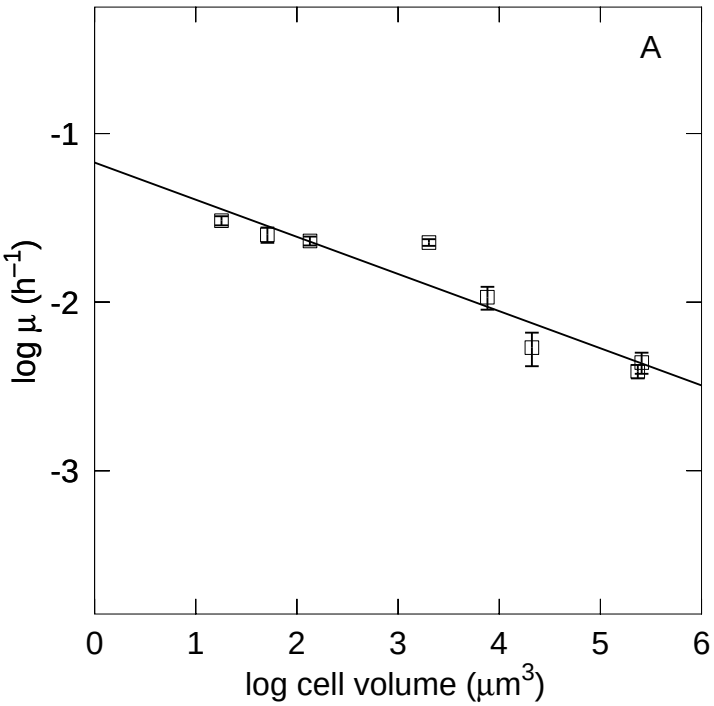

Figure 1A

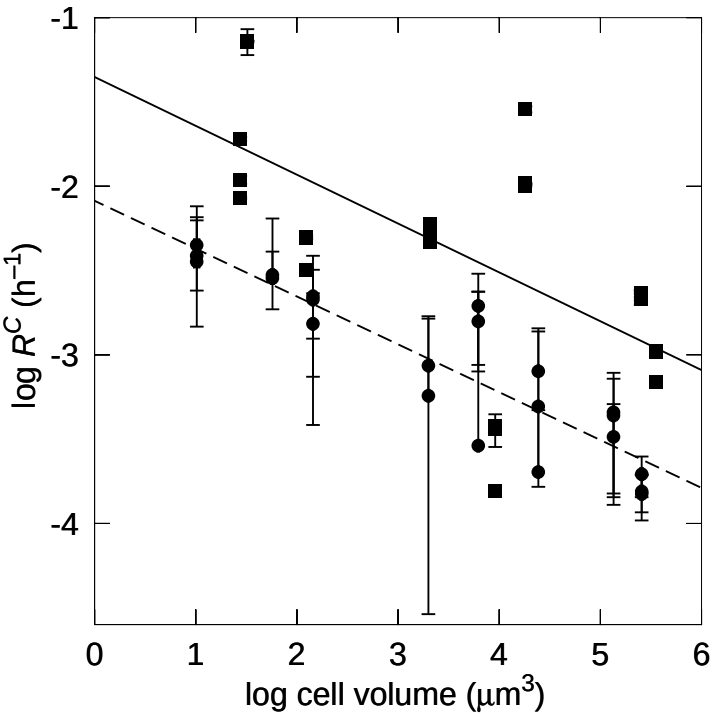

Figure 1B

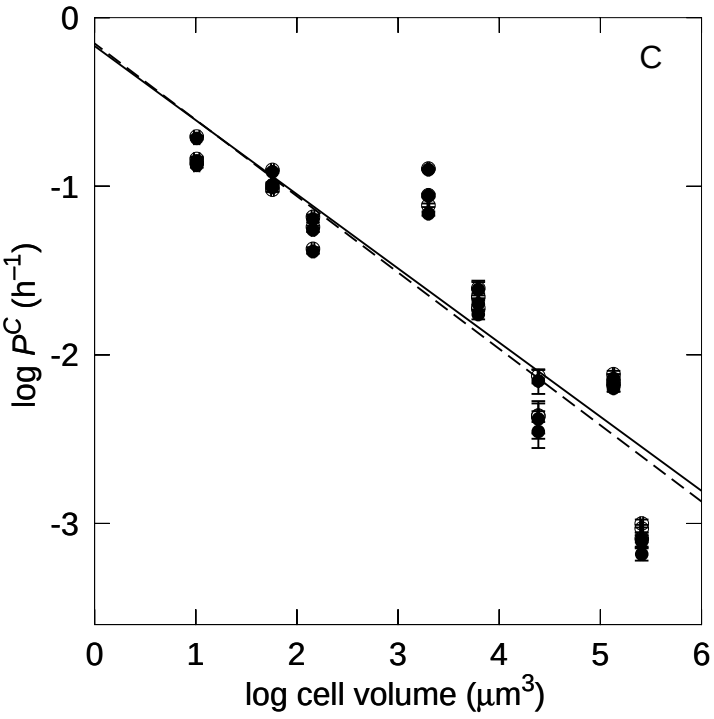

Figure 1C

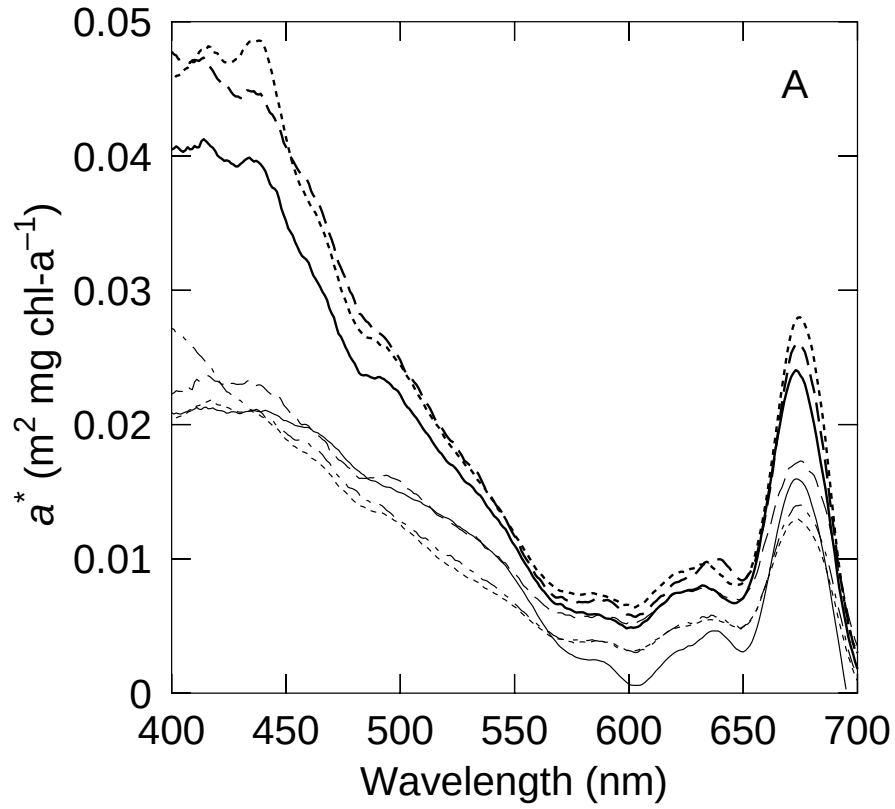
A
0.05
0.04
0.03
0.02
0.01
0
a^* (m^2 mg chl-a^{-1})
400
450
500
550
600
650
700
Wavelength (nm)

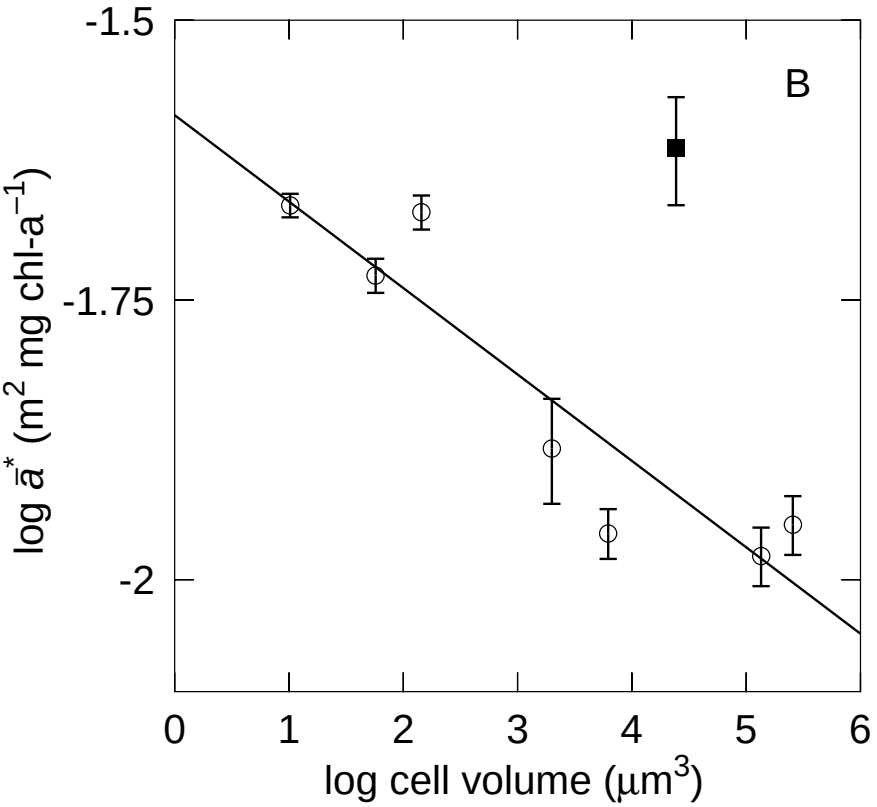
B
-1.5
-1.75
-2
log $\bar{a}^*$ (m^2 mg chl-a^{-1})
0
1
2
3
4
5
6
log cell volume (μm^3)

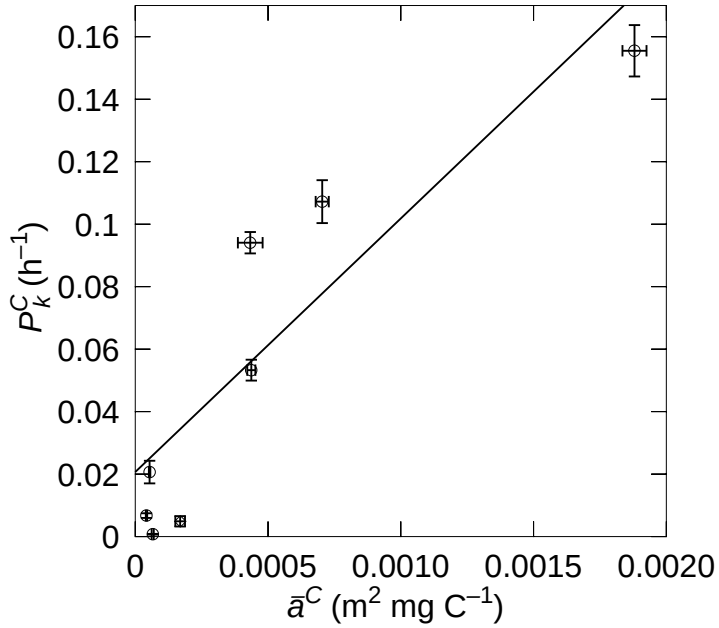
0.16
0.14
0.12
0.1
0.08
0.06
0.04
0.02
0
P_k^C (h^{-1})
0
0.0005
0.0010
0.0015
0.0020
$\bar{a}^C$ (m^2 mg C^{-1})

Figure 3A

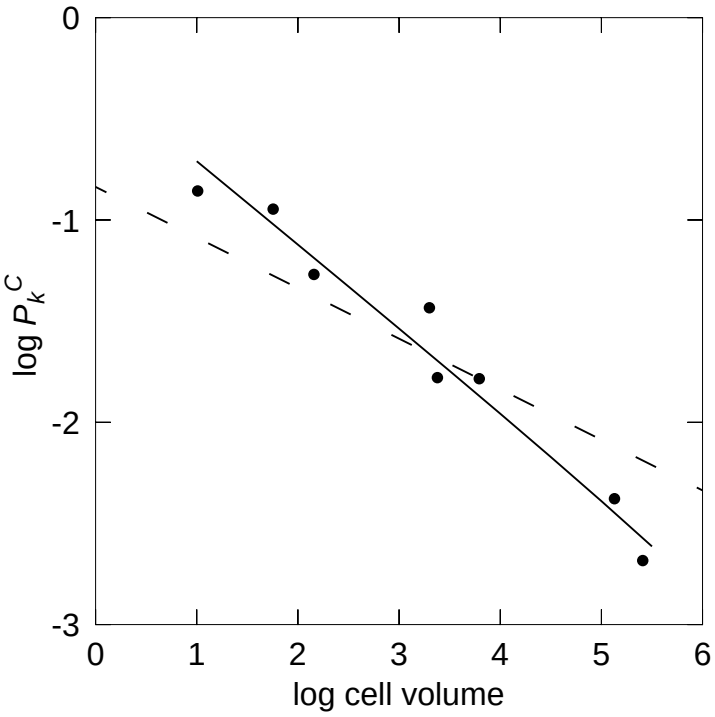

Figure 3B

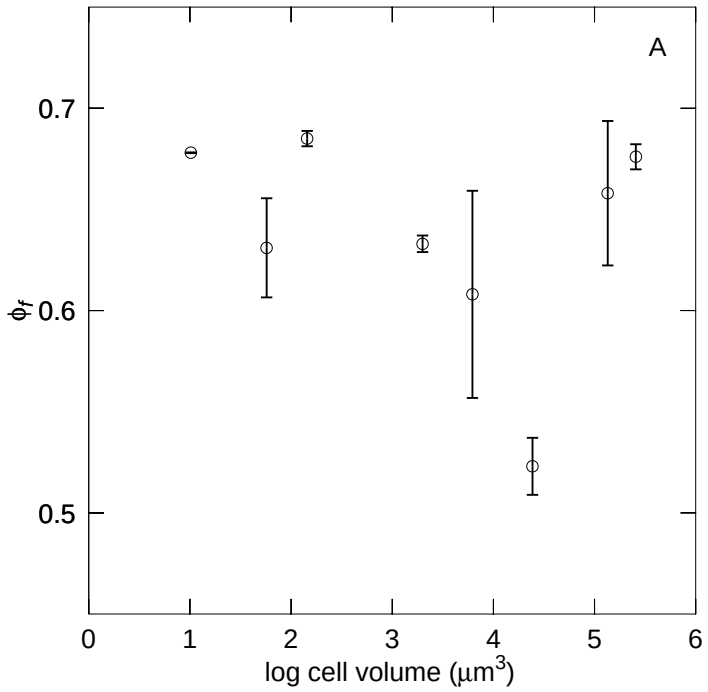

Figure 4A

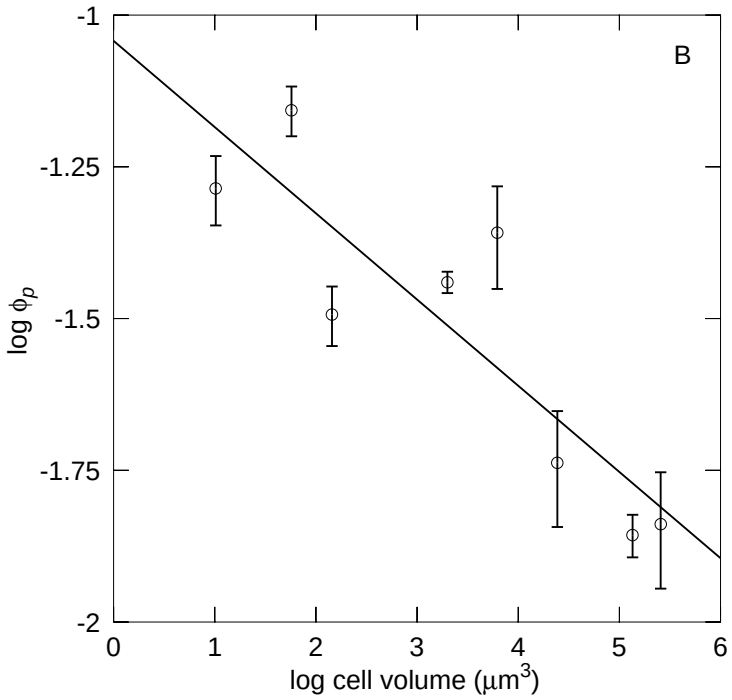

Figure 4B

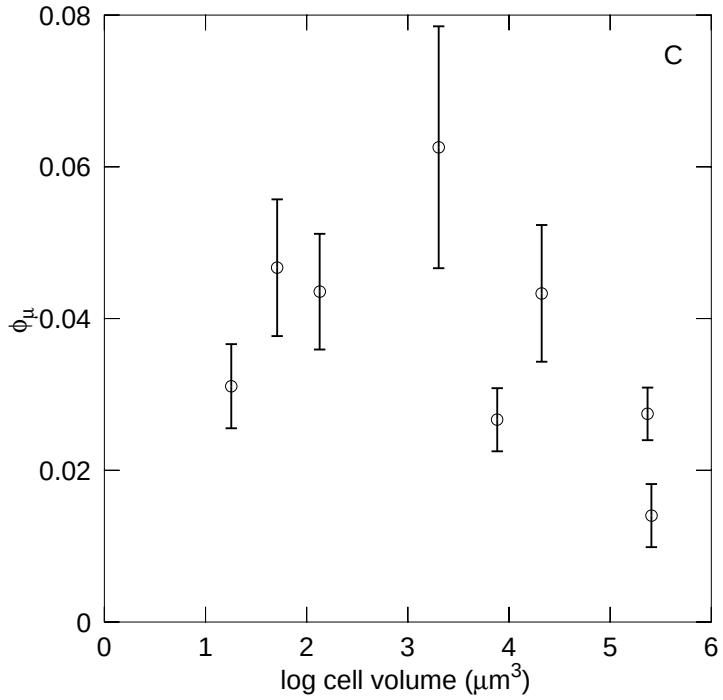

Figure 4C